

The Metrication of Low Probability of Intercept Waveforms

C. Fancey
Canadian Navy
CFB Esquimalt
Esquimalt, British Columbia, Canada
cam_fancey@hotmail.com

C.M. Alabaster
Dept. Informatics & Sensor, Cranfield University
Shrivenham
Oxon, UK, SN6 8LA
c.m.alabaster@cranfield.ac.uk

I. INTRODUCTION

In recent years, military radar operators have been concerned that the transmitted radar signals will beacon the presence of the radar to an enemy. If intercepted, the radar signals alert a target to an attack which could prompt evasive measures or countermeasures to be taken by the target including the possibility of a reprisal attack using an anti-radiation missile. Furthermore, intercepted signals can divulge operating parameters of the radar to the enemy. In response to this low probability of intercept (LPI) requirement, waveforms have been designed to minimize the probability of intercept by an enemy receiver. These are largely based on the use of low peak powers and spread spectrum waveforms offering large processing gains. The interception of signals is a function of both the transmitted radar waveform and the intercept receiver. The aim of this work is to deduce a metric which may be used to quantify and hence compare how “discrete” many of the commonly used LPI radar waveforms actually are. This study considers the following LPI waveforms [1]: Linear Frequency Modulation (LFM), Sinusoidal Frequency Modulation (Sin FM), Poly-Phase Shift Keying (PPSK) techniques including Frank, P1, P2, P3, and P4 codes Costas code Frequency Shift Keying (FSK), and Costas-Barker Hybrid (FSK/PSK). This work represents the first attempt to be published in the open literature to quantify the LPI properties of transmitted radar waveforms. Secure waveform coding strategies to minimize the risk of divulging radar capabilities is known as *low probability of exploitation (LPE)* and is not considered here.

II. CREATION OF METRICATION FORMULA

Since LPI performance represents a probabilistic term, applying a numerical value becomes very difficult. This difficulty arises due to an inherent lack of knowledge of both deterministic and random situational parameters. However, LPI performance can be expressed as a comparison term against other like waveforms by making assumptions as to the purpose of the radar system and that of the enemy Electronic Support Measures (ESM) system. It was determined that the best assumption of radar purpose for this study was an active system using power management techniques attacking a target employing an ESM system. This represents the efforts of a radar system that is forced to remain covert while functioning as an active system in order to accomplish its objective.

This work was based on computer models of the candidate waveforms all having equal energy content and therefore all capable of the same radar detection performance.

The metric used to quantify the LPI performance of waveforms is based on statistical quantities describing the spectral power density of each waveform. The spectrum was derived using a number of closely spaced frequency samples. Two spectra are given in Figure 1 which illustrates the problem of quantifying their LPI qualities.

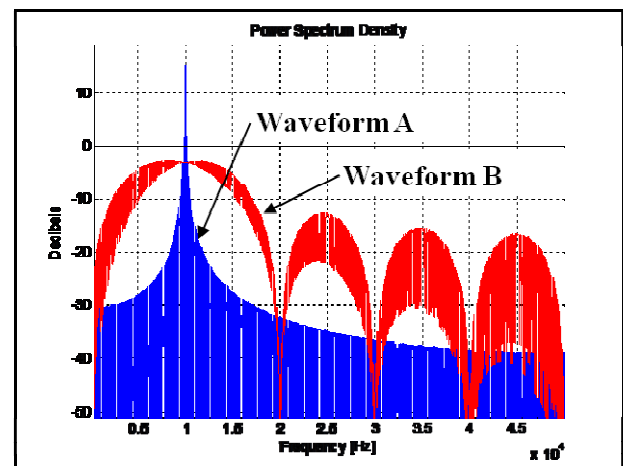


Figure 1 - Power Spectra of Two Waveforms.

If the peak spectral power of the waveform alone is considered, then clearly waveform B, with its peak power level at 20dB below that of waveform A, is more LPI. However, if an ESM receiver with a narrow enough bandwidth is considered, then waveform A is only less LPI than waveform B when the receiver is tuned exactly to 10kHz, 20kHz, and so on.

To help clarify the problem, this study focuses on the interception by a wideband instantaneous receiver ESM System. Although they have very limited direction finding and classifying abilities, these systems provide the greatest threat to LPI waveforms due to their simplicity, low cost and increased probability of detection.

The spectrum was trimmed to include only those samples that cumulatively accounted for 97% of the energy content about the carrier frequency; thus very weak spectral components at large offsets away from the carrier frequency were excluded. This exclusion was necessary during analysis as these waveforms theoretically extend infinitely in spectra at ever decreasing power levels. It was noticed during preliminary analysis attempts that the numerous low-levelled

samples produced unrepresentative statistics for use in this study.

A histogram of the power of the trimmed samples was derived. Example histograms for a polyphase Frank code and linear FM waveforms are given in Figures 2 and 3 below. These are characterised by a peak corresponding to the highest power frequency samples (i.e. samples close to the carrier frequency) and are termed the *Peak Spike* (S_p) and in some cases e.g. the Frank code, Figure 2, a second peak is observed at power levels 10 to 20dB lower than the first.

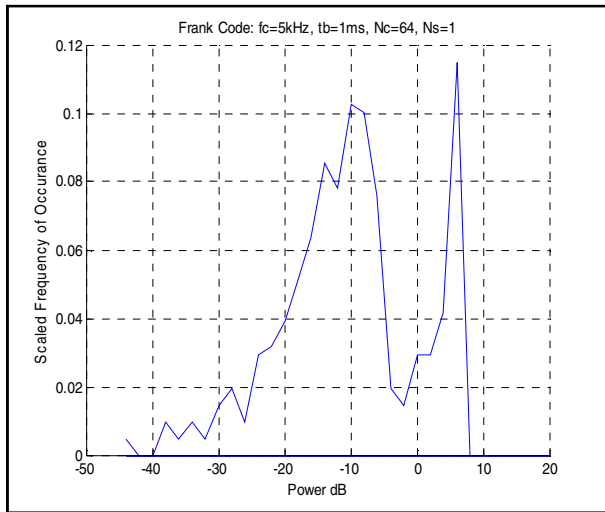


Figure 2 - Histograms of Frank code

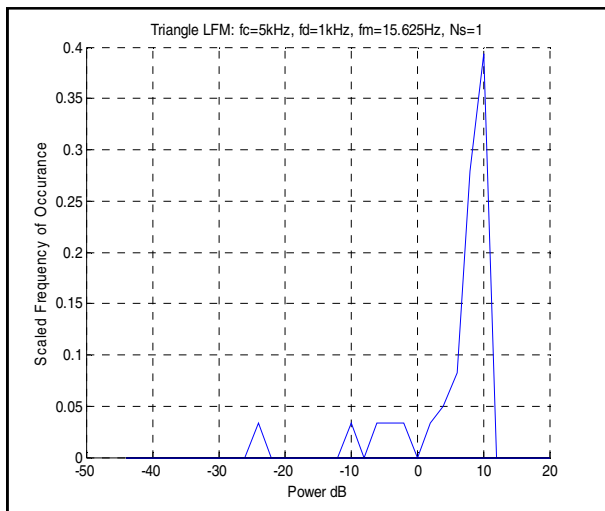


Figure 3 - Histograms of Triangle LFM

It was realized that analysing the transmitted signal itself is not sufficient to create a metrication equation. Consider the examples displayed in Figure 4 and Figure 5. Two transmitted signals, one narrowband and one wideband, with similar peak power are produced as in Figure 4; it is clear that the narrowband signal has a larger peak power and therefore is more susceptible to detection. After applying noise to both waveforms, as in Figure 5, representing the received signal,

we can presume that the addition of noise to the transmitted signals can give the wideband signal a better chance of breaching the ESM's detection threshold over that of the narrowband signal. This gives the wideband signal a better chance of being detected, and therefore a poorer LPI quality. For this reason it was determined that the portions of the signal where the transmitted power is in proximity to the peak power should be considered as a contributor to the detectability of a signal. Conveniently, the peak spike offers a discrete portion of the signal that can satisfy an attempt at metrication.

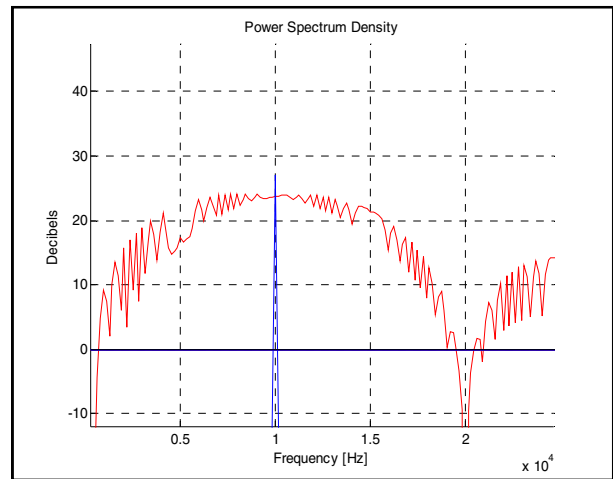


Figure 4 - Two waveforms with similar peak power

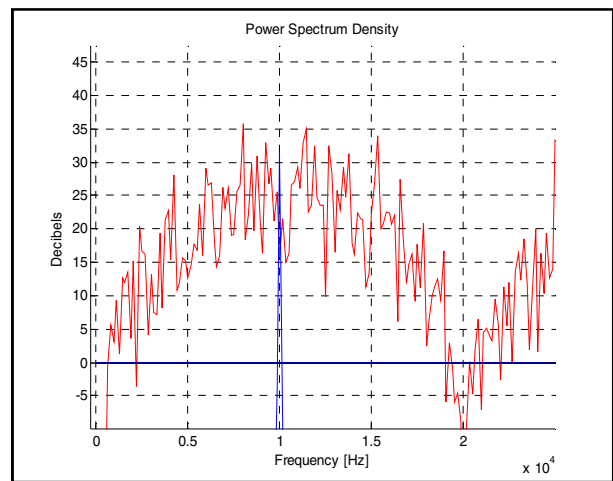


Figure 5 - Addition of noise to two waveforms of similar power

Although the peak power of a signal should be the main consideration, if the peak power of two signals is similar the metrication formula requires a method of distinguishing between the two signals. It was thus determined that a set of LPI waveforms can be ranked by their output signal characteristics using a weighted product of the peak power and the volume of frequencies represented by the peak spike. It was decided to weight the coefficients in order to reflect the importance of the peak power over the peak spike volume. Therefore, an initial weighting of 2 and 1 respectively was

used during the determination of the metrication. However, testing the finalized metrication using an independent simulator, which will be described later, resulted in a difference between the calculated ranking and the simulated results. Therefore a redefinition was given using trial and error to match the simulated results, which produced a revised weighting of 3.2 and 0.6 respectively. The LPI ranking coefficient produced in this study is demonstrated in the following expression:

$$\gamma = P_t^{3.2} * (S_p * \beta)^{0.6} \quad (1)$$

Where γ represents the LPI ranking coefficient of a waveform in a set of waveforms, a lower value of γ represents a better LPI performance. P_t is the peak power, S_p is the normalized frequency of occurrence of output power in the proximity of the peak power level (or the peak spike), and β is the number of samples measured.

III. IMPLEMENTATION

Ten different LPI waveforms (3 LFM, 5 PPSK, and 2 FSK) were simulated, all with an output energy of 1kJ. For each waveform, a histogram of its spectral power density was produced in order to determine the peak power, number of samples and peak spike. This algorithm was executed repeatedly in order to determine a sensitivity to changes in center frequency (f_c), bit time (t_b), code length (N_c) and number of repetitions (N_s).

A. Peak Spike

After using the least squares curve-fitting method on the resulting histogram data points, the normalized magnitude of the peak spike (S_p) of any waveform can be expressed by:

$$S_p = \frac{m_p}{f_c * t_b + c_p} \quad (2)$$

Where m_p and c_p are waveform specific, unitless constants, the values of which can be found in Table 1. Note that the term S_p refers to the y-axis value of the histogram (the frequency of occurrence of the near-peak power levels), and not the x-axis values (the power level of the spike itself).

TABLE 1 - APPROXIMATE VALUES OF PEAK SPIKE (S_p) CONSTANTS

Waveform	m_p	c_p
Sawtooth LFM	0	0.7
Triangle LFM	0	0.4
Sine FM	0	0.25
Frank	0.076	0.106
P1	0.125	0.105
P2	0.067	0.081
P3	0.065	0.11
P4	0.065	0.11
Costas	0.26	0.205
FSK/PSK	0.069	0.04

B. Peak Power

From a statistical analysis of the results it was ascertained that the peak power in dB can be expressed by:

$$P_t \text{ [dB]} = \frac{A_p}{N_c^{n_p}} + B_p \quad (3)$$

Where A_p , B_p and n_p are waveform specific, unitless constants determined by using the least squares curve-fitting method on the statistical results. Their values can be found in Table 2.

TABLE 2 - APPROXIMATE VALUES OF PEAK POWER (P_t) CONSTANTS

Waveform	A_p	B_p	n_p
Sawtooth LFM	2943.7	-2914.2	0.0015
Triangle LFM	-52.26	79.56	-0.062
Sine FM	98.25	-70.99	0.036
Frank	358.47	-330.71	0.012
P1	358.47	-330.71	0.012
P2	124.54	-91.82	0.04
P3	358.47	-330.71	0.012
P4	358.47	-330.71	0.012
Costas	215.68	-189.13	0.016
FSK/PSK	-0.496	15.06	-0.468

C. Number of Samples

The number of samples produced by each waveform was more heavily influenced by N_s and N_c than peak power. This was expected since N_s and N_c directly affects the length of the overall code. The number of samples of a waveform (β) can be expressed as:

$$\beta = A_\beta N_c N_s \left[1 - C_\beta * e^{(n_\beta f_c t_b)} \right] \quad (4)$$

Where A_β and C_β , n_β are waveform specific, unitless constants determined by using the least squares curve-fitting method on the statistical results. Their values can be found in Table 3.

TABLE 3 - APPROXIMATE VALUES OF NUMBER OF SAMPLES (β) CONSTANTS

Waveform	A_β	C_β	n_β
Sawtooth LFM	0.95	0	0
Triangle LFM	0.95	0	0
Sine FM	1.01	0	0
Frank	6.86	0.84	-0.43
P1	6.83	0.94	-0.4
P2	6.7	0.83	-0.33
P3	6.85	0.86	-0.44
P4	6.85	0.86	-0.44
Costas	1.42	0	0
FSK/PSK	13.87	0.88	-0.2

D. LPI Ranking Coefficient (γ)

By substituting (2), (3) and (4) into (1), the initial criterion equation, γ , the metrication of each waveform can be expressed in terms of the input parameters based on their individual sensitivities:

$$\gamma = 10^{\left(\frac{A_p}{N_c^{n_p} + B_p}\right)^{3.125}} * \left[\left(\frac{m_p}{f_c t_b}\right) + c_p \right] \left(A_\beta N_c \left[1 - C_\beta * e^{(n_\beta f_c t_b)} \right] \right)^{0.6} \quad (5)$$

Note that the number of repetitions (N_s) is cancelled out of the metrication equation. As displayed in (2), N_s influences the frequency of occurrence of higher power levels, reducing S_p by a directly inversely proportional amount. However, as displayed in (4), the number of samples (β) is increased by a directly proportional amount. The lack of influence of β on the LPI ranking coefficient (γ), was proven using an independent simulator, discussed later, and has therefore was omitted from the remainder of the study.

IV. RESULTS

By applying the waveform specific constants to each of the ten waveforms using the following four sets of input parameters, the waveforms can be sorted by their LPI ranking (most LPI located at the top), as displayed in Table 4:

- $f_c = 10$ kHz, $t_b = 1$ ms, $N_c = 64$
- $f_c = 10$ kHz, $t_b = 1$ ms, $N_c = 144$
- $f_c = 20$ kHz, $t_b = 1$ ms, $N_c = 64$
- $f_c = 10$ kHz, $t_b = 5$ ms, $N_c = 64$

TABLE 4 - WAVEFORMS RANKED FROM MOST TO LEAST LPI

Waveform	f_c [kHz]	t_b [ms]	N_c	γ LPI ranking coefficient
Frank	10	1	144	2946
P1	10	1	144	2987
P3	10	1	144	2989
P4	10	1	144	2989
Saw-LFM	10	1	144	4291
Tri-LFM	10	1	144	5545
Costas	10	1	144	15746
P1	10	5	64	20050
Frank	10	5	64	20105
Frank	20	1	64	20357
P1	20	1	64	20462
P3	10	5	64	20508
P4	10	5	64	20508
Frank	10	1	64	20627
P3	20	1	64	20721
P4	20	1	64	20721
P1	10	1	64	20929

P3	10	1	64	20944
P4	10	1	64	20944
FSK/PSK	10	1	144	22107
P2	10	1	144	27170
Sin FM	10	1	144	32287
Saw-LFM	10	5	64	36249
Saw-LFM	20	1	64	36249
Saw-LFM	10	1	64	36249
FSK/PSK	10	1	64	44287
FSK/PSK	10	5	64	44328
Tri-LFM	10	5	64	44517
Tri-LFM	20	1	64	44517
Tri-LFM	10	1	64	44517
FSK/PSK	20	1	64	45204
Costas	10	5	64	65416
Costas	20	1	64	65565
Costas	10	1	64	65812
Sin FM	10	5	64	119263
Sin FM	20	1	64	119263
Sin FM	10	1	64	119263
P2	10	5	64	195655
P2	20	1	64	198372
P2	10	1	64	199445

As mentioned earlier in this paper, an independent simulator was created by this author in order to test the LPI ranking coefficient (γ). This simulator pits an average tracking radar against an average ESM system under the circumstances decided upon in the introduction. The system parameters of each system were taken from Stove, Hume, and Baker [2] and can be found in Table 5.

TABLE 5 - SIMULATED SYSTEM PARAMETERS

System Parameter	Attacking Radar	ESM Receiver
Antenna Gain (Transmission)	30dB	-
Antenna Gain (Reception)	30dB	0dB
Integration Gain	4dB	-
Signal To Noise Ratio	15dB	17dB
System Losses	4dB	3dB
Noise Figure	4dB	10dB
Effective Bandwidth	100MHz	200MHz

The simulator assumes the ESM system is utilizing a wideband receiver with its antenna directed towards the attacking radar. The range of the engagement is taken to be the cross-over range (i.e. the range at which the received signal strength is the same upon reception by both the active system and the ESM receiver). The power of the attacking radar is reduced to comply with standard power management

techniques. Finally, White Gaussian Noise is added to each waveform to add the reality of nature.

After inputting two waveforms differing only by one specified parameter, the simulator provides the calculations necessary to determine if the transmitted signal breaches the ESM's detection threshold, indicating an interception. This process is repeated 1000 times for each waveform and the total number of intercepts for each waveform by the ESM receiver are compared to determine which of the two waveforms had a lower probability of detection (or better LPI quality) and this indication of LPI quality is provided to the user.

This simulator was run for a variety of combinations as part of this study. The results of the simulations confirm that the LPI ranking coefficient (γ) at (5) is accurate in 90% of simulated comparisons. The 10% of waveforms that did not conform to the ranking coefficient had nearly identical ranking coefficients and displayed a probability of detection no more than 3.5% in the unexpected direction. This difference is assumed to be attributed to noise.

V. CONCLUSION

The ability to create a metrication equation of LPI performance based on input parameters is certainly feasible, as has been demonstrated here. The main obstacle to confront is the identification of what LPI is and the situational parameters in which it will be used, including system purpose and ESM receiver type.

This formula can be used to rank waveforms for the purpose of LPI system design, but alone it is insufficient in its ability to compare the stealth properties between two separate LPI radar systems. It is also important to re-state that this metrication only refers to the LPI performance of a waveform and not its LPE performance.

As seen in Table 4, this particular metrication formula provides a rank order of waveforms from most to least LPI that is valid given the assumptions made here.

REFERENCES

- [1] Pace, Phillip E. (2004), *Detecting and Classifying Low Probability of Intercept Radar*, Artech House, London.
- [2] Stove, A.G., Hume, A.L. and Baker, C.L. (2004), "Low Probability of Intercept Strategies", *IEE Proceedings – Radar, Sonar and Navigation*, Vol. 151, Issue 5, p.249-260